

# On the stability analysis of optimal state feedbacks as represented by deep neural models

Dario Izzo<sup>\*</sup> and Dharmesh Tailor<sup>†</sup> and Thomas Vasileiou<sup>‡</sup>  
*European Space Agency, Advanced Concepts Team*

## I. Introduction

RECENT research has shown how the optimal feedback control of several non linear systems of interest in aerospace applications can be represented by deep neural architectures [1–3] and trained using techniques including imitation learning, reinforcement learning and evolutionary algorithms. Such deep architectures are here also referred to as Guidance and Control Networks, or G&CNETs. It is difficult to provide theoretical proof on the stability of neurocontrollers in general, and G&CNETs in particular, to perturbations, time delays or model uncertainties or to compute stability margins and trace them back to the network training process or to its architecture. In most cases the analysis of the trained network is performed via Monte Carlo experiments and practitioners renounce to any formal guarantee. This lack of validation naturally leads to skepticism on the use of neurocontrollers, especially in cases where safety and validation are of paramount importance such as is the case, for example, in the space industry.

In an attempt to narrow the gap between deep learning research and control theory, we here make use of automatic differentiation [4] and high order Taylor maps [5] to analyze a generic neurocontroller and we apply fundamentals results in control theory to obtain formal guarantees on its behaviour next to equilibrium points, as well as on its stability to time delays and on its behavior in proximity of a nominal trajectory. After presenting a general methodology, we make use, as a case study, of a simplified, two-dimensional quadcopter dynamics, controlled by a G&CNET trained over power optimal control trajectories to show the potentials of the proposed methodology. All the code and data to reproduce the results in this paper is made available via the github repository <https://github.com/darioizzo/neurostability>.

## II. Stability of neural optimal feedbacks (G&CNETs)

### A. Neural network representation of optimal trajectories

The free-time optimal control problem of steering a nonlinear dynamical system  $\dot{\mathbf{x}} = \mathbf{f}(\mathbf{x}, \mathbf{u})$  from an initial state  $\mathbf{x}_0$  to a target state  $\mathbf{x}_f$  minimizing the functional  $J(\mathbf{x}, \mathbf{u}, t_f) = \int_{t_0}^{t_f} \ell(\mathbf{x}, \mathbf{u}) dt$  admits, under some rather loose assumptions, a unique solution called optimal feedback and here indicated with  $\mathbf{u}^*(\mathbf{x}), t_f^*$  and resulting in the optimal trajectories  $\mathbf{x}^*(t)$ . Whenever the target state is also an equilibrium point for the system under the control  $\mathbf{u}_e$ , that is  $\mathbf{f}(\mathbf{x}_f, \mathbf{u}_e) = \mathbf{0}$ , we extend

---

<sup>\*</sup>Scientific Coordinator, Advanced Concepts Team

<sup>†</sup>Young Graduate Trainee, Advanced Concepts Team

<sup>‡</sup>Research Fellow, Advanced Concepts Team

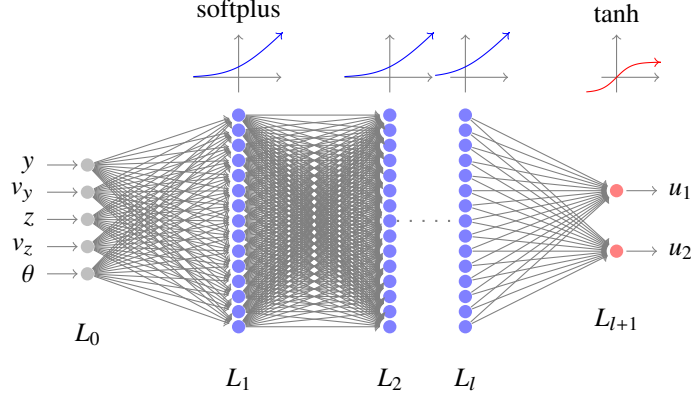


**Fig. 1** The architecture of the G&CNETs  $\mathcal{N}$  studied.

the optimal feedback as follows:  $\mathbf{u}^*(\mathbf{x}_f) = \mathbf{u}_e$ . In other words, the optimal action is to keep being at equilibrium when our initial position is at the equilibrium. In these cases, we also use the symbol  $\mathbf{x}_e$  to denote the final target state. Note that using the value function  $v(\mathbf{x}) = \int_{t_0}^{t_f^*} \ell(\mathbf{x}, \mathbf{u}^*) dt$  as a Lyapunov function candidate, the global asymptotical stability of  $\mathbf{x}_e$  can be proved straight forwardly also from Belmann optimality principle.

**Definition II.1** A G&CNET (Guidance and Control Network) is a type of neuro controller, in particular a deep, artificial, feed forward neural network trained on state-action pairs representing the optimal control actions  $\mathbf{u}^*(\mathbf{x})$ , with respect to the performance index  $J(\mathbf{x}, \mathbf{u}) = \int_{t_0}^{t_f} \ell(\mathbf{x}, \mathbf{u}) dt$ . In other words, a G&CNET is a neural optimal feedback for a non linear dynamical system.

It is interesting that G&CNETS have been shown [1, 2] to be able to learn the policy  $\mathbf{u}^*(\mathbf{x}_f) = \mathbf{u}_e$  even when trained on data that do not contain any equilibrium state-action pair but are derived from optimal control simulations. This is best shown with an example. Consider the one dimensional vertical dynamics of a point mass  $m$  subject to the gravity  $g$  and to a control action  $u \in [-20, 20]$ . A deep network can be trained to approximate the time optimal feedback to reach the origin and would only see, during its training, values for  $u$  that are either -20 or 20 (a consequence of Pontryagin maximum principle [6]), but could still be able to predict that for  $x = 0$  the optimal action is  $u = g$ , a fact the network was never exposed to.

We indicate the optimal state feedback as approximated by a trained deep network with  $\mathcal{N}(\mathbf{x}) \approx \mathbf{u}^*(\mathbf{x})$ , where the symbol  $\mathcal{N}$  reminds us that a deep network is defining the complex relation between inputs and outputs. The resulting non linear dynamical system resulting from the use of the G&CNET can be expressed as:

$$\dot{\mathbf{x}} = \mathbf{f}(\mathbf{x}, \mathcal{N}(\mathbf{x})) \quad (1)$$

The G&CNET  $\mathcal{N}(\mathbf{x})$ , being a deep network, is a complex expression containing the composition of non linearities (i.e. the network activation functions) that layer after layer form a representation of the optimal control actions. Formally,

a G&CNET can be expressed as:

$$\mathcal{N}(\mathbf{x}) : \begin{cases} L_0 = \mathbf{x} \\ L_{i+1} = \sigma_i(\mathbf{W}_i L_i + \mathbf{b}_i), \forall i = 0..l \\ L_{l+1} = \hat{\mathbf{u}}^* \end{cases} \quad (2)$$

where  $L_0 = \mathbf{x}$  is the state vector and  $L_{l+1} = \hat{\mathbf{u}}^*$  the predicted optimal control vector. The weight matrices  $\mathbf{W}_i$  and bias vectors  $\mathbf{b}_i$  are found during the network training and determine the properties both of the resulting controller and the non linear system in Eq.(1). The activation functions  $\sigma_i$  as well as the network dimensions (i.e.  $l$  and the dimensions of weights and biases) are decided before training and constitute the network architecture. When expanded fully, the expression above does not provide much mathematical insight on the resulting control structure nor it provides a straight-forward way to study its stability, margins and, in general, performances. This fact, valid in general for any representation of a control that uses an artificial neural network, gives raise to skepticism on the possibility to use such controllers in applications where the satisfaction of requirements must be proved using formal mathematical tools. Despite its complex form, though, a deep network is a mathematical function in the class  $C^n$ , where  $n$  is the lowest among all the continuity classes of its activation functions  $\sigma_i$ . This simple observation enables us to propose and test new approaches to study the quality of G&CNETs as on-board controllers based on the differentiability of the network outputs.

### 1. Neurocontroller dynamics linearisation

Starting from a generic neurocontrolled system  $\dot{\mathbf{x}} = \mathbf{f}(\mathbf{x}, \mathbf{u})$ ,  $\mathbf{u} = \mathcal{N}(\mathbf{x})$ , we derive, around the point  $\mathbf{x} = \mathbf{x}_e$ , its linearised form  $\dot{\mathbf{x}} = \mathbf{A}\mathbf{x}$ , where  $\mathbf{A}$  is the gradient of the right hand side of the dynamics  $\mathbf{f}$  computed in correspondence to the linearization point, in symbols:  $\mathbf{A} = \nabla \mathbf{f}|_{\mathbf{x}=\mathbf{x}_e}$ . Expanding further the expression, indicating the matrix  $\mathbf{A}$  through its components  $a_{i,j}$  we get:

$$a_{ij} = \frac{df_i}{dx_j} = \frac{\partial f_i}{\partial x_j} + \frac{\partial f_i}{\partial u_k} \left( \frac{\partial \mathcal{N}_k}{\partial x_j} \right). \quad (3)$$

It is clear, from the above expression, that to compute the linear dynamics we need to compute the derivatives of the neural network outputs with respect to its inputs (circled term). This task can be most efficiently solved using automatic differentiation, a technique that is of widespread use in deep learning research as it forms the core of the backpropagation algorithm used to train the network during supervised learning tasks. All main deep learning frameworks (Tensorflow, Pytorch, etc.) are able to compute the requested terms efficiently using backward automatic differentiation and for any network\*. Note that, when computing  $\frac{\partial \mathcal{N}_k}{\partial x_j}$ , discontinuities such as those introduced by ReLU nonlinearities are basically

---

\*We here used pyaudi [7], and in particular its low order forward automated differentiation system implemented with dual numbers

neglected and the various activation functions are thus seen as piece-wise differentiable.

Once  $\mathbf{A}$  is computed, we may then solve the linear eigenvalue problem to find the right eigenvector matrix  $\mathbf{V} = [\mathbf{v}_1, \mathbf{v}_2, \dots]$  and the eigenvalue matrix  $\mathbf{\Lambda}$  such that  $\mathbf{A}\mathbf{V} = \mathbf{V}\mathbf{\Lambda}$ . The dynamics of the neurocontrolled system, next to the equilibrium point, will thus be  $\delta\mathbf{x} = e^{\mathbf{A}t}\delta\mathbf{x}_0$ , having introduced the variable  $\mathbf{x} = \mathbf{x}_e + \delta\mathbf{x}$ . Thus the solution  $\delta\mathbf{x} = e^{\mathbf{A}t}\delta\mathbf{x}_0$  is a linear combination of terms in the form  $e^{-\lambda_i t}$ . The real part of the eigenvalues is then determining the asymptotic behavior of the system, while the imaginary part  $\omega_i$  determines its oscillating behaviour introducing a frequency  $f = \frac{\omega_i}{2\pi}$ . Since G&CNETS are approximations of the optimal control, the analysis can be informative for both the optimal control stability margins as well as the network training quality (i.e. how good an approximation really is).

Next, we investigate the robustness of the neurocontroller with respect to feedback delays, an issue commonly encountered in real-time systems. To this effect, we introduce the time delay  $\tau$  in the system dynamics:

$$\mathbf{x}(t) = \mathbf{f}(\mathbf{x}(t), \mathcal{N}(\mathbf{x}^\tau)) \quad (4)$$

where  $\mathbf{x}^\tau = \mathbf{x}(t - \tau)$ . Essentially, we assume that the current action is calculated based on the system state delayed by  $\tau$ . Also in this case, using automated differentiation it is possible to compute, without introducing any numerical artifact, the linear state space representation:

$$\dot{\delta\mathbf{x}} = \mathbf{A}\delta\mathbf{x} + \mathbf{B}\delta\mathbf{x}^\tau \quad (5)$$

This linear system with time delay has the general solution [8]:  $\delta\mathbf{x}(t) = e^{\mathbf{\Phi}t}\mathbf{x}_0$  where the matrix  $\mathbf{\Phi}$  eigenvalues are obtained from the time-delayed characteristic equation:

$$|\mathbf{A} + \mathbf{B}e^{-\lambda\tau} - \lambda\mathbf{I}| = 0 \quad (6)$$

note that for  $\tau = 0$  (no delay) we recover the stability study of the non delayed system. The solution to the above equation forms the locus root of the system for different delay values. Detecting the first occurrence of the imaginary axes crossing by one of the roots allows to determine the critical time delay,  $\tau^*$ , that destabilizes the system. Unfortunately, the solution to Eq.(6) comes with quite some issues associated to the initial guess and the non linear nature of the equation. While eigenvalue tracking approaches can help alleviate such issues, the resulting numerical methods are somehow cumbersome and inefficient. As a consequence, in this work we use the Pade approximation of order 5 for the time delay, to obtain the initial guess for solving Eq.(6). The time delay in the Laplace domain can be approximated as a rational function of two polynomial of equal degree,  $e^{-s\tau} \approx P(s)/Q(s)$ , where  $s$  is the Laplace variable. Transforming this approximation in the time domain and applying it separately on each state of the original system, the linear system

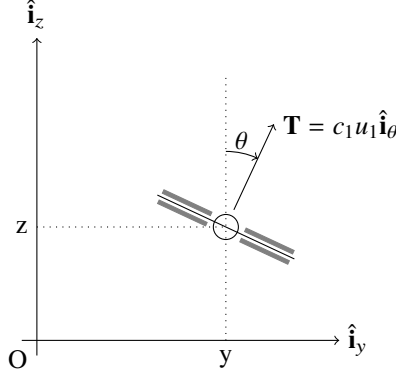


**Fig. 2 The quadcopter system.**

for the delayed state can be written as:

$$\delta \mathbf{x}^\tau \approx \mathbf{C}_p \mathbf{x}_p + \mathbf{D}_p \delta \mathbf{x} \quad (7)$$

$$\dot{\mathbf{x}}_p = \mathbf{A}_p \mathbf{x}_p + \mathbf{B}_p \delta \mathbf{x} \quad (8)$$

where the matrices  $\mathbf{A}_p$ ,  $\mathbf{B}_p$ ,  $\mathbf{C}_p$  and  $\mathbf{D}_p$  depend on  $\tau$  and  $\mathbf{x}_p$  are internal states of the system. The input to this linear system is the current state  $\delta \mathbf{x}$  and the output is the approximation of the delayed state  $\delta \mathbf{x}^\tau$ . Interconnecting the approximation Eq.(7-8) with the delayed system Eq.(5), results on a linear system

$$\begin{bmatrix} \delta \dot{\mathbf{x}} \\ \dot{\mathbf{x}}_p \end{bmatrix} = \begin{bmatrix} \mathbf{A} + \mathbf{B}\mathbf{D}_p & \mathbf{B}\mathbf{C}_p \\ \mathbf{B}_p & \mathbf{A}_p \end{bmatrix} \begin{bmatrix} \delta \mathbf{x} \\ \mathbf{x}_p \end{bmatrix}$$

with an augmented state. An estimate for  $\tau^*$  is then obtained by tracking the eigenvalues of the augmented system matrix.

## 2. High order Taylor maps of neurocontrolled trajectories

In those cases where  $\mathcal{N}(\mathbf{x})$  is at least  $C^n$  we can use differential algebraic techniques [9] to expand into Taylor polynomials of order  $n$  any function that depends on the network outputs. These expansion can be used to analyze the behavior of the neurocontroller to parametric uncertainty and determine the space of stable perturbations. In the following, we look into perturbations of the initial state  $\mathbf{x}_0$  with respect to a given nominal trajectory, although perturbations with respect to any other model parameters are also possible. In particular, consider the solution to the initial value problem associated to Eq.(1):

$$\mathbf{x}(t) = \Phi_{\mathcal{N}}(t, \mathbf{x}_0)$$

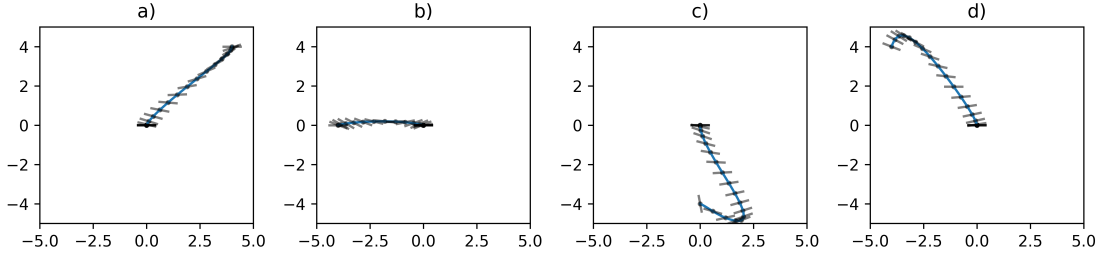


**Fig. 3 Four different manoeuvres of the quadcopter controlled by a G&CNET. The corresponding optimal trajectories are not visible due to overlap to the ones reported.**

where the subscript reminds us of the neural network dependency. For any fixed time  $t = T$ , and reference point  $\mathbf{x}_0$ , we consider the function  $\mathbf{x}_T = \Phi_N(T, \mathbf{x}_0)$  and we compute its Taylor representation (or map)  $\mathbf{x}_T \approx \mathcal{M}_{\mathbf{x}_0}^{n,T}(\delta\mathbf{x})$ . The map  $\mathcal{M}_{\mathbf{x}_0}^{n,T}$  describes, to order  $n$  and at time  $T$ , the solution to the initial value problem with initial condition  $\bar{\mathbf{x}}_0 = \mathbf{x}_0 + \delta\mathbf{x}$ . Such representations are called Taylor models, or high order Taylor maps in the literature (see [10] for a nice recent overview of the technique or [5] for an earlier work) and are here computed using the open source python package `pyaudi` [7] developed at the European Space Agency. The map  $\mathcal{M}_{\mathbf{x}_0}^{n,T}$  is a  $n$ -th order Taylor polynomial in  $\delta\mathbf{x}$  and can be used to study the neural controller behaviour around a nominal trajectory since it represents an explicit form of the solution of Eq.(1), at least in a neighbourhood of the nominal trajectory starting at  $\mathbf{x}_0$ . Indeed for  $T \rightarrow \infty$ , or in practice sufficiently large, if the equilibrium  $\mathbf{x}_e$  is globally asymptotically stable, then  $\mathcal{M}_{\mathbf{x}_0}^{n,\infty} = \mathbf{x}_e$ , a fact that is easily checked once the map  $\mathcal{M}$  is computed and also allows to guarantee, mathematically, that the neural controller is able to drive the system to the desired state from all initial values in some neighbourhood of  $\mathbf{x}_0$ . For the computation of such maps, we numerically integrate, using a Runge-Kutta-Fehlberg scheme, the dynamics of the system from  $\bar{\mathbf{x}}_0 = \mathbf{x}_0 + \delta\mathbf{x}$  up to time  $T$  using the algebra of truncated Taylor polynomials. We make use of the software package `pyaudi` [7] and implement our own version of a Runge-Kutta-Fehlberg adaptive step scheme.

To summarize, the use of the techniques introduced above allows to establish, in a system controlled by a G&CNET, mathematical guarantees a) on the local stability of the equilibrium point  $\mathbf{x}_e$ , b) on the linear time delay margin of the system and c) on the stability of some nominal trajectory originating from  $\mathbf{x}_0$ . Considering that the controller is a deep feed forward neural network, these guarantees acquire a great importance as they allow to trust to a higher degree the decisions made by artificial neural networks which are often seen as a dangerous black-box elements in the control loop. In the next section we will apply the above ideas and method on a practical test case: the two-dimensional dynamics of a quadcopter.

### III. Numerical experiments

#### A. The quadcopter model

Consider the system shown in Fig. (2) representing a quadcopter whose two-dimensional dynamics is defined by the following set of ordinary differential equations:

$$\begin{cases} \dot{\mathbf{r}} = \mathbf{v} \\ \dot{\mathbf{v}} = c_1 \frac{u_1}{m} \hat{\mathbf{i}}_\theta + \mathbf{g} - \frac{1}{2} \mathbf{v} \\ \dot{\theta} = c_2 u_2 \end{cases} \quad (9)$$

The quadcopter state includes its position  $\mathbf{r} = (y, z)$ , its velocity  $\mathbf{v} = (v_y, v_z)$  and its orientation  $\theta$ . We also refer to the state using the variable  $\mathbf{x} = [\mathbf{r}, \mathbf{v}, \theta]$  and to the controls using the variable  $\mathbf{u} = [u_1, u_2]$ . In the rest of this note, we will use data from the @Parrot Bebop drone as an example. The mass of the quadcopter is set to be  $m = 0.38905$  [kg] and the acceleration due to the Earth's gravity is  $\mathbf{g} = (0, -g)$  where  $g = 9.81$  [m/s<sup>2</sup>]. Note that the dynamics of the quad is also perturbed by a drag term and its coefficient is set to  $\frac{1}{2}$ . The control  $u_1 \in [0.05, 1]$  corresponds to a thrust action applied along the direction  $\hat{\mathbf{i}}_\theta = [\sin \theta, \cos \theta]$  bounded by a maximum magnitude  $c_1 = 9.1$  [N] and a minimum magnitude of  $0.05c_1 = 1$  [N]. The control  $u_2 \in [-1, 1]$  models a quadcopter pitch rate bounded by  $c_2 = 35$  [rad/s].

For the above non linear dynamical system we consider the optimal control problem of steering the state from any initial state to the target state,  $\mathbf{r}_t = (0, 0)$ ,  $\mathbf{v}_t = (0, 0)$  and  $\theta = 0$  minimizing the cost function:

$$J = \int_0^{t_f} (c_1^2 u_1^2 + c_2^2 u_2^2) dt \quad (10)$$

and we train several G&CNETS  $\mathcal{N}(\mathbf{x})$  to represent the optimal state feedback  $\mathbf{u}^*(\mathbf{x})$  for the problem above. As this paper is not focused on the network training in itself, rather on evaluating the resulting control performances, we point to previous work for further details on G&CNETs learning [1, 2, 11, 12].

The basic architecture for the networks  $\mathcal{N}_l^n$  we consider is shown in Figure 1 together with the nonlinearities used. All networks are feed forward neural networks having  $l$  layers of  $n$  softplus nonlinearities (i.e.  $\sigma_i = \log(1 + \exp(\cdot))$ ) and a  $\sigma_i = \tanh(\cdot)$  output nonlinearity. Since  $u_1 \in [0.05, 1]$ , we scale the corresponding output unit range to match this domain. The use of softplus units in G&CNETS is introduced with the idea to create network outputs of class  $C^\infty$  and thus avoid problems that could arise deploying differential algebraic methods to compute Taylor models or even the simple linearization around the equilibrium point. In our experiments, the softplus units resulted also in consistently better training losses when compared to the tanh or ReLu units used in previous work [2]. We tested various network architectures, containing 1 to 9 hidden layers and 50 to 200 neurons per layer. We report in Tab.(1) the various mean squared errors obtained on a test set made of 1,180,000 optimal state action pairs after training on 9,440,000 optimal

**Table 1 Mean Average Error (x1000) and number of parameters for the various trained G&CNETS  $\mathcal{N}_l^n$** 

		$n$		
		50	100	200
$l$	1	31.7 / 402	30.3 / 802	28.2 / 1602
	2	11.3 / 2952	8.4 / 10902	7.3 / 41802
	3	7.9 / 5502	7.2 / 21002	6.6 / 82002
	4	7.5 / 8052	6.1 / 31102	5.9 / 122202
	5	7.9 / 10602	6.1 / 41202	5.9 / 162402
	6	6.5 / 13152	6.4 / 51302	5.9 / 202602
	7	6.3 / 15702	5.9 / 61402	5.9 / 242802
	8	6.6 / 18252	6.0 / 71502	6.2 / 283002
	9	7.4 / 20802	6.0 / 81602	6.0 / 323202

**Table 2 Stability margins for various neurocontrollers**

	$\zeta_{10\%}$	$T$	$\tau^*$		$\zeta_{10\%}$	$T$	$\tau^*$		$\zeta_{10\%}$	$T$	$\tau^*$
$\mathcal{N}_1^{50}$	2.27s	2.41s	0.137s	$\mathcal{N}_1^{100}$	1.97s	2.48s	0.140s	$\mathcal{N}_1^{200}$	1.64s	2.56s	0.134s
$\mathcal{N}_2^{50}$	1.66s	0.00s	0.034s	$\mathcal{N}_2^{100}$	2.09s	3.80s	0.029s	$\mathcal{N}_2^{200}$	1.94s	3.17s	0.026s
$\mathcal{N}_3^{50}$	1.73s	2.63s	0.023s	$\mathcal{N}_3^{100}$	1.80s	3.59s	0.022s	$\mathcal{N}_3^{200}$	1.39s	3.21s	0.024s
$\mathcal{N}_4^{50}$	1.26s	2.52s	0.026s	$\mathcal{N}_4^{100}$	2.54s	0.00s	0.032s	$\mathcal{N}_4^{200}$	2.33s	3.90s	0.050s
$\mathcal{N}_5^{50}$	1.19s	3.32s	0.037s	$\mathcal{N}_5^{100}$	1.52s	0.00s	0.037s	$\mathcal{N}_5^{200}$	1.18s	4.37s	0.060s
$\mathcal{N}_6^{50}$	0.89s	2.07s	0.039s	$\mathcal{N}_6^{100}$	1.40s	1.19s	0.091s	$\mathcal{N}_6^{200}$	1.87s	5.59s	0.043s
$\mathcal{N}_7^{50}$	0.59s	2.00s	0.056s	$\mathcal{N}_7^{100}$	1.70s	1.06s	0.071s	$\mathcal{N}_7^{200}$	1.30s	1.23s	0.050s
$\mathcal{N}_8^{50}$	0.71s	8.34s	0.069s	$\mathcal{N}_8^{100}$	1.25s	2.18s	0.059s	$\mathcal{N}_8^{200}$	1.39s	1.30s	0.042s
$\mathcal{N}_9^{50}$	0.78s	2.68s	0.091s	$\mathcal{N}_9^{100}$	2.13s	0.56s	0.047s	$\mathcal{N}_9^{200}$	0.89s	0.54s	0.024s

state action pairs.

Since the networks are only but approximations to the underlying optimal feedback  $\mathbf{u}^*(\mathbf{x})$ , it is to be expected that the differential equations expressed in Eq.(9), when using  $\mathbf{u} = \mathcal{N}_l^n(\mathbf{x})$ , will not have an equilibrium point exactly at the origin. Before applying the analysis here introduced to study the various neurocontroller performances, we thus correct all networks first by computing  $\hat{\mathbf{x}}_l^n$  as the equilibrium point of the system  $\dot{\mathbf{x}} = \mathbf{f}(\mathbf{x}, \mathcal{N}_l^n(\mathbf{x}))$  and then by translating our axis as to place  $\hat{\mathbf{x}}_l^n$  in the origin. Such a shift was, in our test case, ranging from  $10^{-2}$  to  $10^{-3}$ , confirming the good quality obtained during training. We also show, in Figure 3, an example of the trajectories resulting from the use of  $\mathcal{N}_3^{100}$  to control the quadcopter dynamics starting from four different  $\tau$  initial conditions. The optimal trajectories, as evaluated solving the optimal control problem, overlap exactly with the ones produced by the network.

### 1. Hovering stability and stability to time delay

After shifting our axis, the dynamical system  $\dot{\mathbf{x}} = \mathbf{f}(\mathbf{x}, \mathcal{N}(\mathbf{x}))$  has in the origin  $\mathbf{O}$  its equilibrium point and thus  $\mathcal{N}(\mathbf{O}) = [u_1, u_2] = [\frac{gm}{c_1}, 0]$ . This corresponds, in our case study, to the quadcopter hovering over the origin and cancelling exactly the gravitational pull with its upward thrust. We thus proceed to study the behavior of the quadcopter

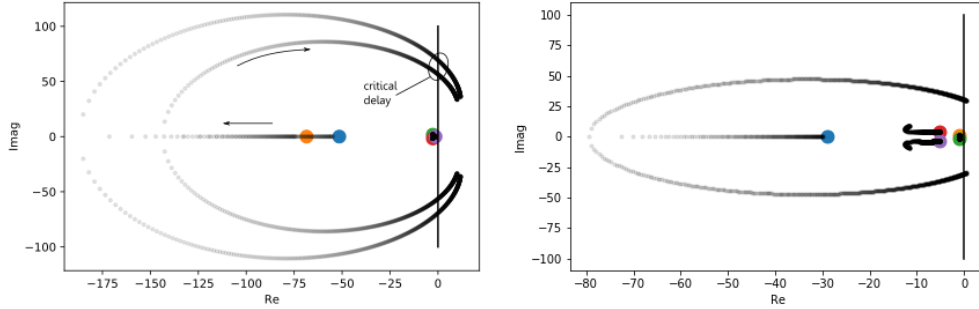


**Fig. 4** Root locus for  $\mathcal{N}_{100}^3$  (left) and  $\mathcal{N}_{200}^4$  (right). The arrows indicate the movement of the eigenvalues for increasing  $\tau$ .

close to the hovering conditions by computing all the eigenvalues  $\lambda_i = \alpha_i + j\beta_i$  of the linear dynamics matrix  $\mathbf{A}$  computed from Eq.(3) for each of the trained networks. In all cases, the modes computed resulted to be stable, that is  $\alpha_i < 0, \forall i = 1..5$ , proving that all trained networks result in a stable dynamics near the hovering position. For each eigenvalue we computed the decay time,  $\zeta_{10\%_i} = \frac{\ln(0.1)}{\alpha_i}$ , which is defined as the time the envelope associated to the  $i$ -th mode takes to decay to 10% of its starting value, and the oscillating period,  $T_i = \frac{2\pi}{\beta_i}$ , associated to the  $i$ -th mode. In Table (2) we report the largest values for  $\zeta_{10\%}$  and  $T$  for each network  $\mathcal{N}_i^n$ . At most one pair of complex conjugate eigenvalues was present in all cases tested.

We then perform the analysis of the time delayed system solving Eq.(6) for different values of the time delay  $\tau$  and thus producing a root locus which we show in Fig.(4) for two different networks:  $\mathcal{N}_{100}^3$  and  $\mathcal{N}_{200}^4$ . The eigenvalues of the non delayed system are also shown. It can be seen from the plots that time delays have, initially, a stabilizing effect on the most stable roots which later give raise to instability crossing the imaginary axis. The computed values for  $\tau^*$  are reported in Tab.(2).

It seems clear that, while deeper and larger networks result in improved representations of the optimal feedback  $\mathbf{u}^*$  (the mean squared error decreases significantly with the network depth and size, Tab.(1)), there is no clear relation between the neurocontroller behaviour in a neighbourhood of the equilibrium point and the network architecture. The only exception being shallow networks (i.e. networks with only one layer) that seem to have a consistently higher stability margin to time delay  $\tau$ . While this is an advantage, shallow networks also have a very large mean squared error which indicates that their approximation of the underlying optimal control structure  $u^*$  is rather poor, as shown in Tab.(1). This behaviour is worth being discussed briefly. The equilibrium point is, for the optimal feedback  $\mathbf{u}^*$  the network seek to learn, a discontinuity point where the value of  $u_1$  becomes instantaneously  $\frac{gm}{c_1}$  from its value at the last instant of the optimal trajectory. As a consequence, the optimal dynamics  $\mathbf{x}^*$ , in a neighbourhood of the origin does not follow exponential laws of the type  $\exp(-ct)$  and thus cannot be described by a linear system. While deeper and larger networks do approximate the optimal feedback to a higher degree, they also are continuous functions and thus allow for a linear analysis of the resulting dynamics next to the origin. This cannot be correlated to the optimal dynamics  $\mathbf{x}^*$  that

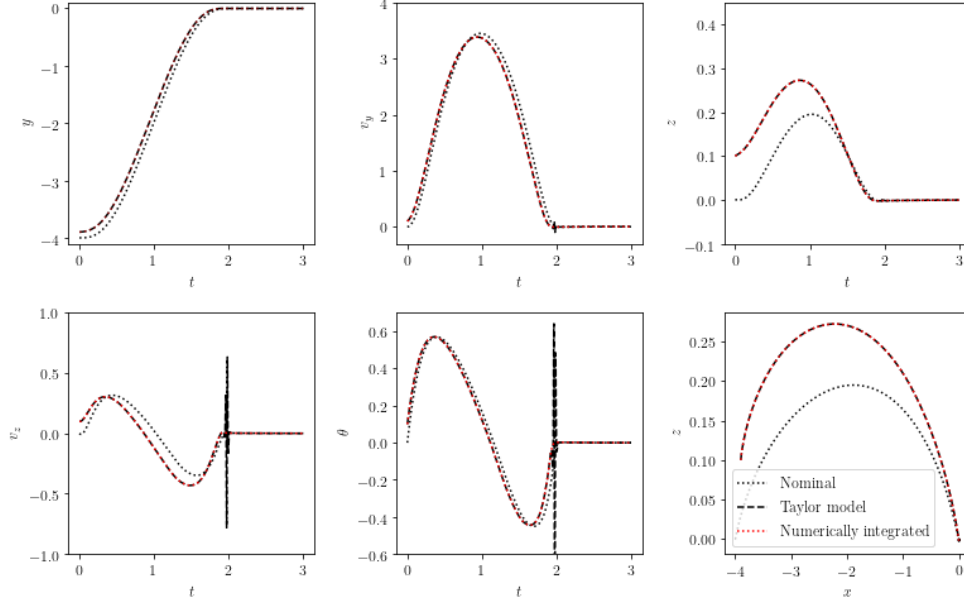


**Fig. 5** Taylor model representation of an optimal trajectory .  $\mathcal{M}_{\mathbf{x}_0}^{7,i}$  is shown for  $\delta \mathbf{x} = [0.1, 0.1, 0.1, 0.1, 0.1]$ .

does not admit a linear representation. The linear analysis of the neurocontroller behaviour next to the equilibrium point is thus useful to introduce formal stability guarantees, but cannot be used as an alternative metric to the mean squared error to rank the network training quality. The question on how to drive the network training as to obtain a final system meeting predefined requirements on various margins, remains an open issue.

## 2. Trajectory stability

Let us consider, as an example, the quadcopter trajectory resulting from the neurocontroller  $\mathcal{N}_{100}^3$  and the initial condition  $\mathbf{x}_0 = [-4, 0, 0, 0, 0]$ . The trajectory, also shown in Fig.(3b), is a translation manoeuvre where the quadcopter changes its position horizontally by 4 meters. We want to study the stability of such a nominal trajectory with respect to perturbations of the initial conditions  $\bar{\mathbf{x}}_0 = \mathbf{x}_0 + \delta \mathbf{x}$ . In particular we would like to have some type of formal guarantee on the neurocontroller being able to still bring the quadcopter to the final target state for all  $\bar{\mathbf{x}}_0$  in some ball  $B_r$ . In order to estimate the radius of  $B_r$ , we expand the quadcopter trajectory as a high-order Taylor maps, written in the Einstein notation:

$$x_{T,i} = \Phi_{N,i}(T, \mathbf{x}_0) + a_{1,ij}\delta x_j + a_{2,ijk}\delta x_j\delta x_k + a_{3,ijkl}\delta x_j\delta x_k\delta x_l + \dots + \mathcal{O}(n+1) \quad (11)$$

where  $x_{T,i}$ ,  $\Phi_{N,i}(T, \mathbf{x}_0)$  and  $\delta x_i$  denote the  $i$ -th component of  $\mathbf{x}_T$ ,  $\Phi_N(T, \mathbf{x}_0)$  and  $\delta \mathbf{x}$  respectively. The terms  $a_1$ ,  $a_2$  and  $a_3$  are components of the gradient, the Hessian and the third-order partial derivatives tensors. In the case of a quadcopter, since the state has a dimension of five, the resulting map will contain 5, 20, 55, 125, 251, 461, 791 terms as the order grows from the first. Clearly, if the quadcopter has to reach and maintain its hovering position starting from a perturbed

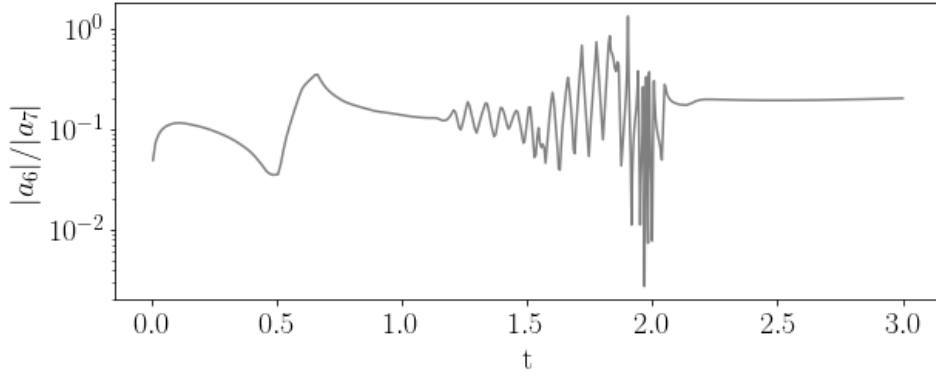


**Fig. 6 Proxy for the convergence radius computed on  $\mathcal{M}^{7,i}$  and on its  $v_z$  component.**

initial state in the ball  $B_r$ , the series represented formally in Eq.(11) must converge for all  $\delta\mathbf{x} \in B_r$  to the equilibrium point. When this is the case, a formal guarantee on the stability of the nominal trajectory is obtained. Since we cannot compute the Taylor model for  $T \rightarrow \infty$ , we stop at  $T = \frac{3}{2}t_f^*$  (with  $t_f^*$  representing the time of the optimal manoeuvre) letting the system enough time to reach the equilibrium position and stabilize itself. In the case of our nominal trajectory this corresponds to  $\approx 3$  sec. We thus compute at  $T = 3$  sec. the Taylor model of the state at order  $n = 7$ .

When computing the map at  $T$  running the Runge-Kutta-Fehlberg scheme, we also obtain, at no added computational costs, the maps at all previous times  $T_i$  requested by the numerical integrator and we thus write  $\mathcal{M}_{\mathbf{x}_0}^{n,i}(\delta\mathbf{x})$  to indicate the map of order  $n$  at the time  $T_i$ . The collection of these maps represent a complete explicit description of the neurocontrolled trajectories and thus of the optimal dynamics  $\mathbf{x}^*$  close to the nominal trajectory. The question on how big a ball  $B_r$  they actually describe rests on the analysis of the convergence of the various Taylor series. As an example, we show in Fig. (5) the quadcopter state during the nominal trajectory and the state predicted by the various maps  $\mathcal{M}_{\mathbf{x}_0}^{7,i}(\delta\mathbf{x})$  for a rather large perturbation  $\delta\mathbf{x} = [0.1, 0.1, 0.1, 0.1, 0.1]$ . We also show the ground truth as computed by numerical integration of Eq. 1 from point  $\bar{\mathbf{x}}_0$ . Interestingly, the map is representing the  $\delta\mathbf{x}$  perturbed optimal trajectory quite accurately for many time instants, but it also fails catastrophically for  $t \approx 2$  sec., where the selected perturbation is evidently larger than the corresponding map convergence radius. It is the estimate of such radius that is therefore of great interest. In order to obtain this estimate, we take the norm of the series in Eq.(11) and by applying the triangle inequality and the properties of the induced matrix norms, we write:

$$\|\mathbf{x}_T\| \leq \|\Phi_{\mathcal{N}}(T, \mathbf{x}_0)\| + \|\mathbf{A}_1\| \|\delta\mathbf{x}_1\| + \|\mathbf{A}_2\| \|\delta\mathbf{x}_2\| + \|\mathbf{A}_3\| \|\delta\mathbf{x}_3\| + \dots$$

To write the previous equation in a matrix-vector notation, we have unfolded the tensors such that all the partial derivatives corresponding to the same  $\Phi_{\mathcal{N},i}$  are in the same row, e.g. for  $\mathbf{A}_{2,ij} = a_{2,ikl}$  and  $\mathbf{A}_{3,ij} = a_{3,iklm}$  with  $k = (j-1)$

$\text{mod } 5 + 1$ ,  $l = (j - 1) \div 5 + 1$  and  $m = (j - 1) \div 5^2 + 1$ ,  $j = 1, 2, \dots, 25$  and  $j = 1, 2, \dots, 125$  in the each matrix respectively. We apply the same unfolding to the vectors  $\delta \mathbf{x}_2$  and  $\delta \mathbf{x}_3$  as  $\delta \mathbf{x}_{2,j} = \delta x_k \delta x_l$  and  $\delta \mathbf{x}_{3,j} = \delta x_k \delta x_l \delta x_m$  where the indices  $k$ ,  $l$  and  $m$  depend on  $j$  as before. It is easy to show that  $\|\delta \mathbf{x}_2\| = \|\delta \mathbf{x}\|^2$  and  $\|\delta \mathbf{x}_3\| = \|\delta \mathbf{x}\|^3$  under any  $p$ -norm. As a result, we are able to rewrite for example the map  $\mathcal{M}_{\mathbf{x}_0}^{7,i} \leq \sum_{i=0}^7 a_i \epsilon^i$ , where  $a_i$  are the corresponding matrix norms and  $\|\delta \mathbf{x}\| = \epsilon$ , and study the convergence of this series to obtain a conservative estimate of the radius of convergence of our expansion. For the numerical calculations we use the  $\infty$ -norm, namely the largest absolute element for vectors and maximum absolute row sum for matrices. In the infinite series, the magnitude of the  $\lim_{n \rightarrow \infty} \frac{|a_{n+1}|}{|a_n|}$ , if existing, is the largest  $\epsilon$  allowing to prove the series convergence. This is readily seen by applying the ratio convergence test (D'Alembert's criterion) to the series:  $\epsilon \lim_{n \rightarrow \infty} \frac{|a_{n+1}|}{|a_n|} < 1$ . When this limit exists, it also implies:  $\epsilon < \lim_{n \rightarrow \infty} \frac{|a_n|}{|a_{n+1}|}$ . Since it is impossible to numerically compute such a limit in our case, we propose to use  $\frac{|a_6|}{|a_7|}$  as a proxy for it (higher orders are also possible). In Fig.(6) we show this estimate for the radius of convergence in logarithmic scale and for the map  $\mathcal{M}^{7,i}$  showing how, for  $T_i \approx 2$  sec. the Taylor map radius of convergence estimate is indeed problematic but it eventually stabilizes at  $T_i = 3$  sec. around a high value, hinting at a good stability margin for the nominal trajectory. Note however that the surrogate for the radius of convergence here proposed and used does not imply any formal mathematical guarantee and is only proposed as an indicator.

## IV. Conclusions

We proposed a new general methodology to analyse the behaviour of neurocontrollers. Our method allows to study the neurocontrolled feedback dynamics in proximity of equilibrium points by deriving linear stability margins as well as time delay margins. We then propose the use of high order Taylor models to study the robustness of a nominal trajectory to perturbations on its initial conditions. The methodology is applied successfully to the study case of the Parrot Bebop quadcopter dynamics where we show, for several G&CNETs having diverse depth and complexity, the formal stability guarantees for the neurocontrolled hovering behaviour as well for the stability of a test nominal manoeuvre. We found that as soon as the network is deep, i.e. has more than one hidden layer, there seem to be no relation between the linear stability margins obtained and the network architecture. We also found that the computed Taylor model of the state describes well the neurocontrolled trajectories in a neighbourhood of the nominal trajectory and we propose a method to estimate the size of said neighbourhood. Our results constitute a first step to increase the trust on neurocontrolled systems by narrowing the gap between control theory and deep learning.

## References

- [1] Sánchez-Sánchez, C., Izzo, D., and Hennes, D., "Learning the optimal state-feedback using deep networks," *Computational Intelligence (SSCI), 2016 IEEE Symposium Series on*, IEEE, 2016, pp. 1–8.
- [2] Sánchez-Sánchez, C., and Izzo, D., "Real-time optimal control via Deep Neural Networks: study on landing problems," *Journal*

- of Guidance, Control, and Dynamics*, Vol. 41, No. 5, 2018, pp. 1122–1135.
- [3] Levine, S., “Exploring Deep and Recurrent Architectures for Optimal Control,” *CoRR*, Vol. abs/1311.1761, 2013. URL <http://arxiv.org/abs/1311.1761>.
- [4] Griewank, A., et al., “On automatic differentiation,” *Mathematical Programming: recent developments and applications*, Vol. 6, No. 6, 1989, pp. 83–107.
- [5] Berz, M., and Makino, K., “Verified integration of ODEs and flows using differential algebraic methods on high-order Taylor models,” *Reliable Computing*, Vol. 4, No. 4, 1998, pp. 361–369.
- [6] Pontryagin, L. S., *Mathematical theory of optimal processes*, CRC Press, 1987.
- [7] Izzo, D., and Biscani, F., “audi/pyaudi,” , Oct. 2018. doi:10.5281/zenodo.1442738, URL <https://doi.org/10.5281/zenodo.1442738>.
- [8] Luo, A. C., *Periodic flows to chaos in time-delay systems*, Vol. 16, Springer, 2016.
- [9] Berz, A., “Differential algebraic description of beam dynamics to very high orders,” *Part. Accel.*, Vol. 24, No. SSC-152, 1988, pp. 109–124.
- [10] Armellin, R., Di Lizia, P., Bernelli-Zazzera, F., and Berz, M., “Asteroid close encounters characterization using differential algebra: the case of Apophis,” *Celestial Mechanics and Dynamical Astronomy*, Vol. 107, No. 4, 2010, pp. 451–470.
- [11] Izzo, D., Sprague, C., and Tailor, D., “Machine learning and evolutionary techniques in interplanetary trajectory design,” , 2018.
- [12] Sanchez-Sanchez, C., Izzo, D., and Hennes, D., “Optimal real-time landing using deep networks,” *Proceedings of the Sixth International Conference on Astrodynamics Tools and Techniques, ICATT*, Vol. 12, No. Aug, 2016, pp. 2493–2537.